Check for updates

Anti-counterfeiting fiber system with near-infrared wavelength selectivity based on photothermal and thermochromic dyes†

Su Jeong Choi, [iD] ‡[a] Eun Jeong Seo, [iD] [a] Hyoung Eun Bae,[a] Hyo Cheol Jung,[a] Sang Ho Lee, [iD] [a] Jin Chul Kim, [iD] [a] Yu Jin Jung,[a] Jong S. Park,[b] Ji-Eun Jeong*[a] and Young Il Park [iD] *[a]

Anti-counterfeiting (ACF) technology plays a crucial role in distinguishing genuine products from counterfeits, as well as in identity verification. Moreover, it serves as a protective measure for safeguarding the rights of individuals, companies, and governments. In this study, a high-level ACF technology was developed using a color-conversion system based on the photothermal effect of near-infrared (NIR) wavelengths. Diimonium dye (DID), which is a photothermal dye, was selected because it is an NIR absorbing dye with over 98% transparency in the visible light (vis) region. Due to the photothermal properties of DID, the temperature increased to approximately 65 °C at 1064 nm and 39 °C at 808 nm, respectively. Additionally, we employed a donor–acceptor Stenhouse adduct dye, a thermochromic dye, which exhibits reversible color change due to heat (red color) and light (colorless). Our ACF technology was applied to the brand-protecting fiber utilizing the difference in photothermal temperature according to the NIR wavelength. We successfully implemented anti-counterfeit clothing using alphabet K labels that could distinguish between genuine and counterfeit products by irradiating with specific NIR wavelengths.

1. Introduction

Anti-counterfeiting (ACF) technology serves a crucial role in safeguarding various products and brands, including clothing, shoes, watches, banknotes, passports, and identity document (ID) cards. Moreover, it is applied to secure the supply chains of raw product materials, such as genuine gasoline and recycled fibers. As a result, businesses and governments should possess the necessary security technologies to thwart intellectual property theft.[1-3]

ACF technology is classified into three levels (Levels 1 to 3) depending on the security level, encompassing overt (Level 1), covert (Level 2), and forensic (Level 3), where higher levels indicate higher security levels. Security Level 1 (overt) technologies are observable with the naked eye without specialized equipment and rely on absorption and reflection in the vis region. Representative examples include photonic crystals and color-change/luminescent materials.[3,4] Thus, there is no requirement for a separate light source or detector. Security Level 2 (covert) technologies are employed for ACF purposes with automatic inspection devices, which are widely used for verifying passports and ID cards. Representative techniques involve the use of red-, blue-, and green-fluorescent materials in the vis region. Therefore, only a general light is required, eliminating the need for specialized detection equipment. Security Level 3 (forensic) technologies necessitate specialized equipment for detection and are primarily used to protect central banks and their brands.[5,6] In addition to a corresponding detector, they require a light source that can selectively provide a special wavelength. As mentioned previously, numerous ACF technologies were developed based on specific wavelength absorption, reflection, and emission characteristics. The ACF level was determined based on the light source and detection equipment used.[7,8]

Research on ACF systems using near-infrared (NIR) wavelengths allows for the implementation of a high-level security system using invisible light sources instead of vis wavelengths. However, expensive detection equipment are required to observe NIR absorption or emission. Therefore, in this study, we attempted to implement an ACF fiber system operating in the NIR region by utilizing an NIR excitation source at a certain wavelength, thus sidestepping the need for costly detection systems. By integrating photothermal and thermochromic dyes,

[a]Research Center for Green Fine Chemicals, Korea Research Institute of Chemical Technology, Ulsan 44412, Republic of Korea. E-mail: jieunj@krict.re.kr; ypark@krict.re.kr

[b]Department of Organic Material Science and Engineering, Pusan National University, Busan, 46241, Republic of Korea

‡ These authors contributed equally to this work.

the proposed ACF fiber system functions effectively at a specific NIR wavelength absorbed by photothermal dye. Sequential color change of thermochromic dyes enables the observation of ACF results with the naked eye, without the use of costly equipment, despite the high security level of forensics.

This paper presents a straightforward approach to an ACF system capable of color conversion upon NIR irradiation at specific wavelengths based on NIR-absorbing photothermal and thermochromic dyes. Photothermal dyes with NIR absorption were selected based on the following criteria: (1) light absorption over 1000 nm: no interference with fiber colors; (2) transparency: to hide the use of security materials; and (3) excellent photothermal properties: for the rapid activation of thermochromic dyes. Diimonium dye (DID), which is a typical NIR-absorbing dye, was selected as the photothermal dye for the proposed ACF system due to its high transparency in the vis region and efficient photothermal properties.[9–11] Various NIR wavelengths can be used by other NIR dyes with photothermal properties, for example, phthalocyanine, squarylium, dithiolene complexes, and cyanine.[12–15] In particular, the combination of two or more photothermal dyes with different NIR absorption wavelengths can be used as a wavelength-based ACF code that is unique to a specific company brand or central bank. In tandem with photothermal dyes, thermochromic dyes were selected for the following properties. (1) Color developed by heat; (2) returns to colorless state under vis; and (3) repeatable color change. Spiropyran derivatives are well-known thermochromic dyes; however, they are colored when light is applied and lose color when heated, thus rendering them difficult to use in ACF applications.[16] Thermochromic xanthene derivatives are not suitable for the proposed strategy because they exhibit an irreversible color change upon heating.[17] In this study, we introduced a donor–acceptor Stenhouse adduct (DASA) dye, which exhibits a reversible color change property, wherein it is colored and colorless when exposed to heat and light, respectively.[18–21] Finally, the proposed ACF system was implemented on highly flexible fibers that could be applied to labels or clothes with versatile shapes and patterns, effectively enhancing brand protection, as shown in Fig. 1.

2. Materials and methods

2.1. Materials

The following chemicals and reagents were purchased from Sigma-Aldrich: 4-bromo-N,N-dibutylmaime, tri-$tert$-butylphosphine (P(t-Bu)$_3$), potassium persulfate, sodium $tert$-butoxide (NaOtBu), lithium bis(oxalate)borate, diethylaminoethanol (EtOH), dichloromethane (DCM), tetrahydrofuran (THF), furfural, dimethylformamide (DMF), poly(methyl methacrylate) (PMMA, average M_W: ~120 000). In addition, 1,3-dimethylbarbituric acid, 1,4-aminobenzene were purchased from TCI, and tri(dibenzylideneacetone)dipalladium(0)(Pd$_2$(dba)$_3$) was purchased from Strem Chemicals. All the reagents were used without further purification.

2.2. Characterization and property of DID and DASA

The overall synthesis process is illustrated in Scheme S1.† The structures of photothermal dyes and thermochromic dyes were confirmed by proton nuclear magnetic resonance (^{1}H-NMR) and gas chromatography mass spectrometry (GC-MS). The ^{1}H-NMR spectra were obtained using a Bruker Ultrashield 300 MHz spectrometer. Ultraviolet-vis-NIR (UV-vis-NIR) absorbance and transmittance spectra in the vis region were recorded using
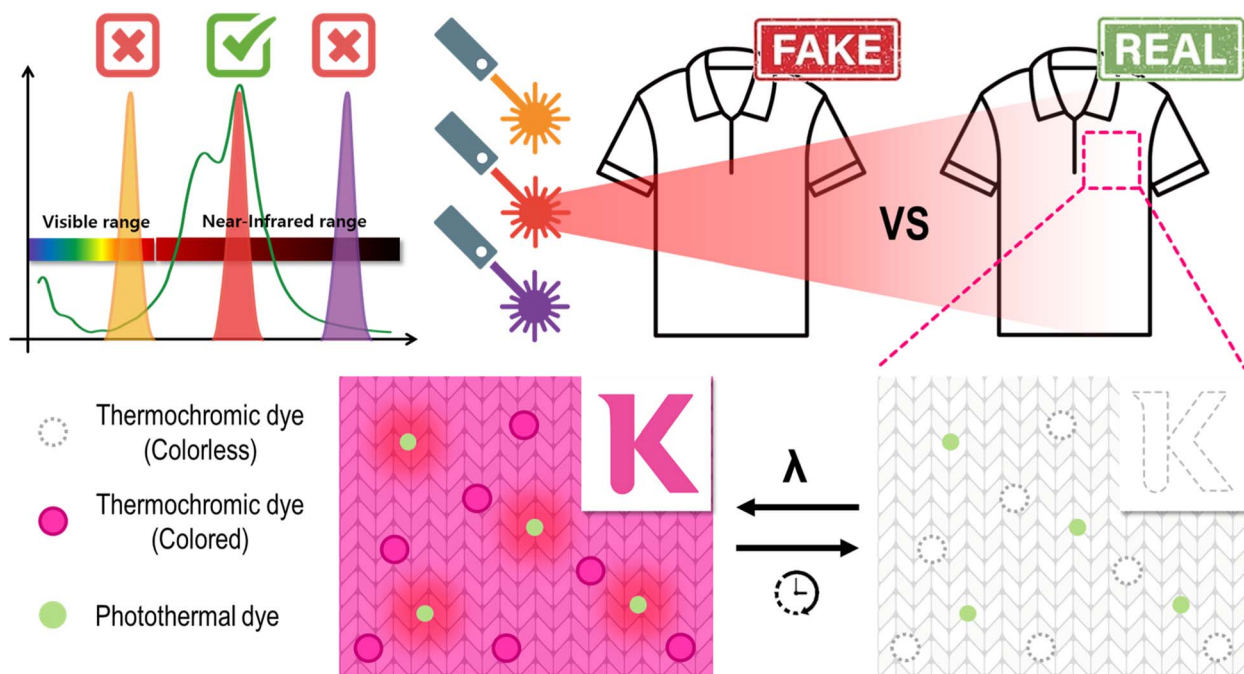

Fig. 1 Schematic illustration of thermochromic dye according to the photothermal dye effect.

a JASCO V-700 spectrometer (1 cm cuvette cell). The reflectance was measured using an ellipsometer (Horiba UVISEL IHR320) at an angle of 75° within the spectral range of 350–820 nm. Photothermal measurements were performed using a 1064 nm laser NIR device (ADR-1805 controller). The laser intensity was adjusted using a ThoElabs PM100D instrument. The temperature changes were observed using a portable thermal imaging camera (FLIR E8 model).

For synthesizing $N1,N1'$-(1,4-phenylene)bis($N4,N4$-dibutyl-$N1$-(4-(dibutylamino)phenyl)benzene-1,4-diamine), place tris(dibenzylideneacetone)dipalladium(0) 0.24 mmol, tri-*tert*-butylphosphine 0.37 mmol in a 2-neck 100 ml flask and stir at room temperature for 10 minutes using 20 ml toluene as a solvent. Add 4-bromoaniline 9.24 mmol and stir at room temperature for another 10 minutes, then add 1,4-aminobenzene 1.85 mmol and sodium *tert*-butoxide 21.6 mmol and stir at 110 °C for 15 hours. The reaction product is cooled to room temperature, extracted with ethyl acetate, moisture removed with sodium sulfate, filtered, and the solvent is completely distilled off using a vacuum distillation device. Dissolve the concentrated

compound in 50 ml of DMF, add 150 ml of isopropyl alcohol, stir for 1 hour at 0 °C, filter the recrystallized compound, and wash with methanol 2 to 3 times to obtain brown powder compound 1 (82%) was obtained.

For the synthesis of bisoxalatobolate N,N,N',N'-tetrakis(p-dibutylaminophenyl)-p-phenylendiimonium (diimmoium dye, DID), 0.2 g (0.22 mmol) of the synthesized 1 and 0.12 g (0.54 mmol) of lithium bis(oxalate)borate were placed in a 2-neck 100 ml of round flask and 10 ml of DCM, and 5 ml of EtOH were stirred at 70 °C for 4 h. After dissolving 0.1 g (0.33 mmol) of potassium persulfate in 4 ml of H_2O, the mixture was stirred for an additional 2 h. The resultant solution underwent extraction using H_2O and DCM, with subsequent removal of H_2O using sodium sulfate, followed by filtration and complete distillation of the organic solvent using a vacuum distillation device. The concentrated compound was washed 2–3 times with n-hexane and dried to obtain 0.26 g of compound (2), as shown in Fig. S1.† The yield was 85%, and the ^1H NMR (acetone-d6, 300 MHz) showed δ 6.90–6.71 (br d, 12H), 6.62–6.57 (br d, 8H), 3.28 (s, 16H), 1.55 (br m, 16H), 1.36 (br m, 16H), and 0.93 (br m, 24H).
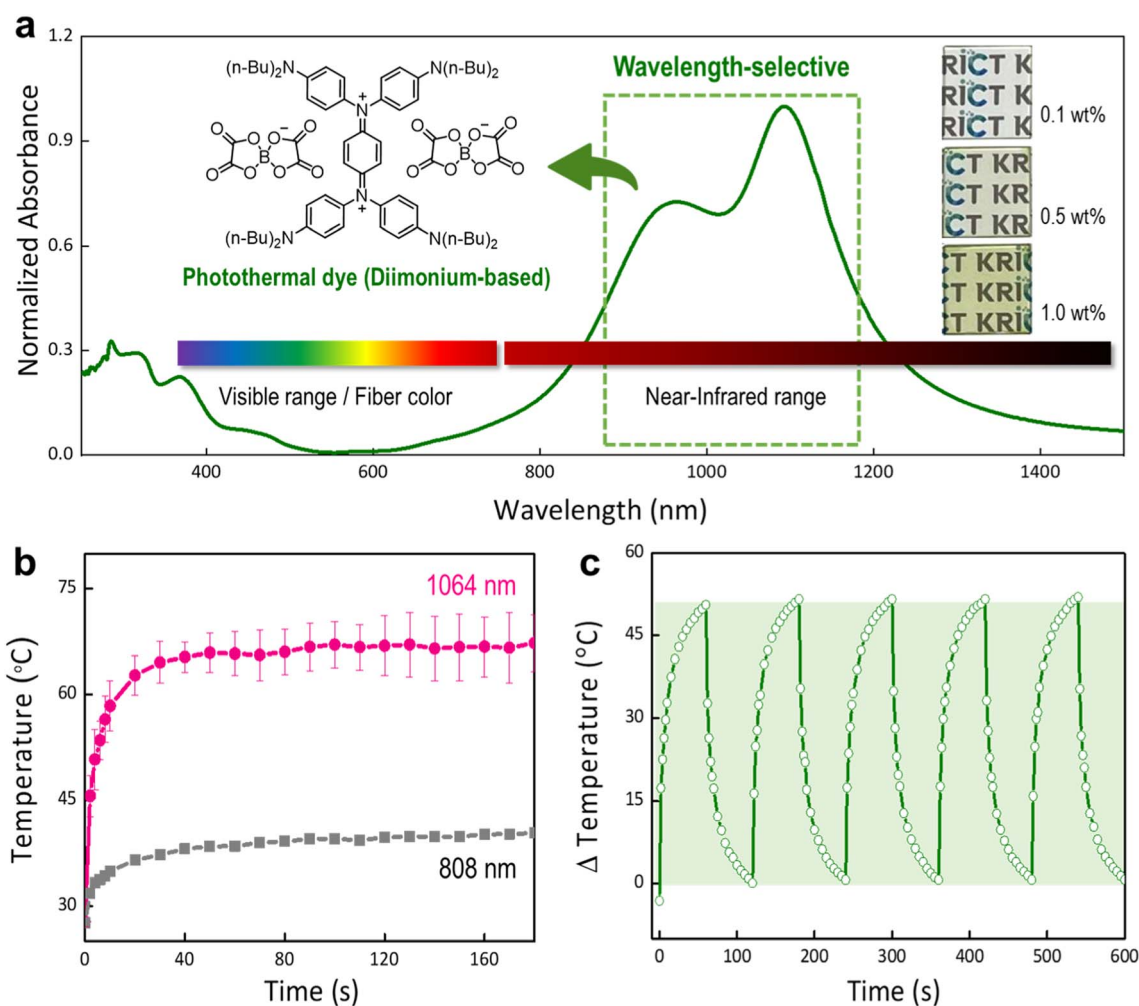

Fig. 2 (a) Normalized UV-vis. absorption spectrum of diimonium dye (insert: chemical structure and diimonium dye coated film). (b) Photothermal property of 0.1 wt% diimonium dye coated film at 1064 nm and 808 nm. (c) Photothermal stability of diimonium dye coated film at 1064 nm.

For the synthesis of 5-(furan-2-ylmethylene)-1,3-dimethylpyrimidine-2,4,6(1H,3H,5H)-trione, 2-furaldehyde and 1,3-dimethylbarbituric acid are mixed with water and stirred at room temperature for two hours. Filter the yellow solid mixture and wash it several times with cold water. After extraction with MC/NaHSO$_3$, the organic layer is completely separated using MgSO$_4$. The compound is obtained by drying all solvents through reduced pressure distillation.

For synthesizing 5-((2Z,4E)-5-(diethylamino)-2-hydroxypenta-2,4-dien-1-ylidene)-1,3-dimethylpyrimidine-2,4,6(1H,3H,5H)-trione (DASA), 10 mmol of compound (3) and 10 mmol of diethylamine were dissolved in 20 ml of DCM. The mixture was stirred at room temperature for 30 min and then cooled to 0 °C, followed by stirring for an additional 30 min. After distilling the solvent of the mixture under reduced pressure, the mixture was precipitated with cold ether to obtain compound (4) in Fig. S2.† The yield was 71% and the ^{1}H NMR (CDCl3, 300 MHz) showed δ 12.58 (s, 1H), 7.25 (s, 1H), 7.19 (d, 1H), 6.75 (d, 1H), 6.10 (tri, 1H), 3.52 (m, 4H), 3.38 (s, 6H), and 1.36 (m, 6H).

2.3. Fiber dyeing procedure

In this study, color and temperature changes were observed during dyeing based on the concentrations of photothermal and thermochromic dyes as variables. The clean cotton fibers were completely precipitated in water with dissolved DASA and soaked for 3 h. The cotton fibers were naturally dried at room temperature for 4 h to allow for complete drying. The completely dried DASA-dyed cotton fibers were precipitated in a solvent containing the photothermal dye, immersed for a short time-period to prevent the dissolution of the dyed DASA, and then removed. The cotton fiber was allowed to dry naturally to completion at room temperature for 1 h.

2.4. Photothermal film manufacturing

Photothermal measurements were performed using an ADR-1805 controller. To evaluate the photothermal performance, NIR lasers with output wavelengths of 1064 nm (IR1064T3H-1000, Shanghai Laser & Optics Century Co., Ltd. (SLOC)) and 808 nm (IRM808TA, Shanghai Laser & Optics Century Co., Ltd. (SLOC)) were used. The laser intensity was monitored using a PM100D optical power and energy meter (Thorlabs) equipped with a thermal power sensor head (S425C; Thorlabs). The temperature changes were observed using a portable thermal imaging camera (FLIR E8).

To measure the fibers, the temperature changes were confirmed using the T_{max} function of a thermal imaging camera
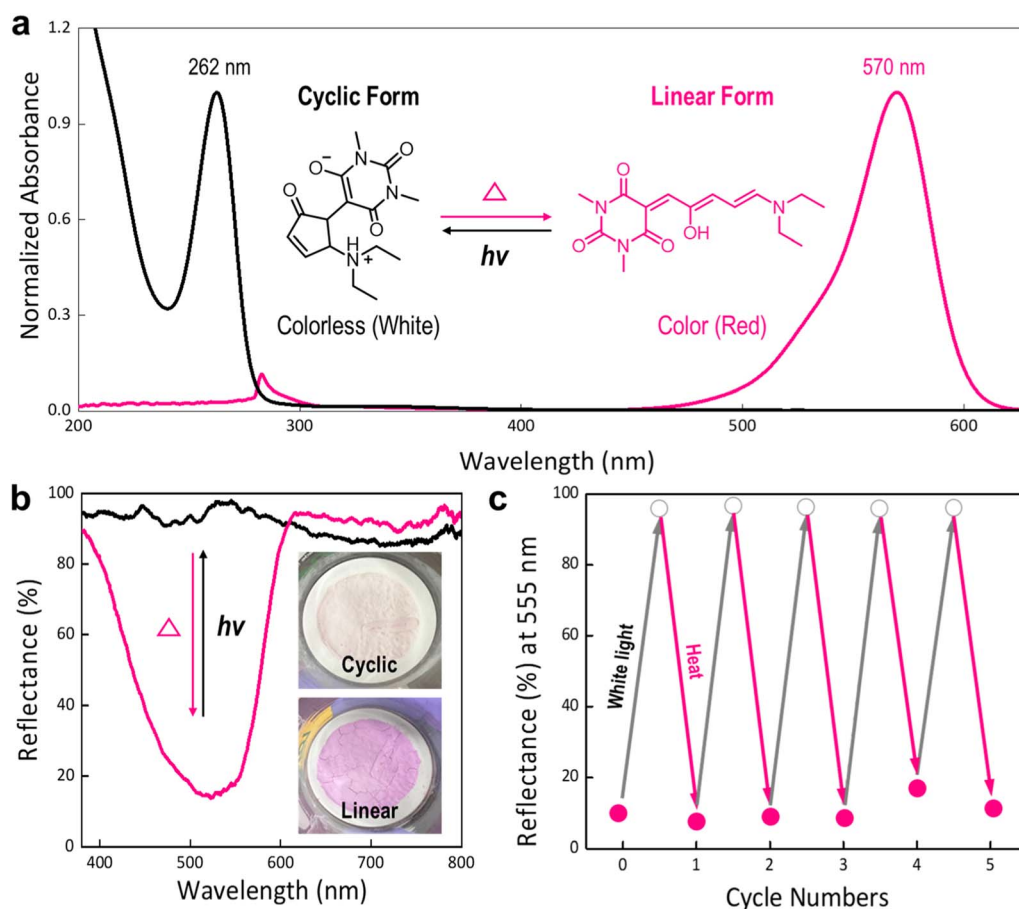

Fig. 3 (a) Normalized UV-vis. spectra of cyclic form in H$_2$O solution and linear form of DASA in toluene solution (b) reflectance of DASA cyclic form under irradiating white light and DASA linear form by applying heat in solid phase (c) repeatability of DASA during five white light/heat cycles (white light, not a specific wavelength, was irradiated at an intensity of 0.1 W/observe color change in a 50 degree oven).
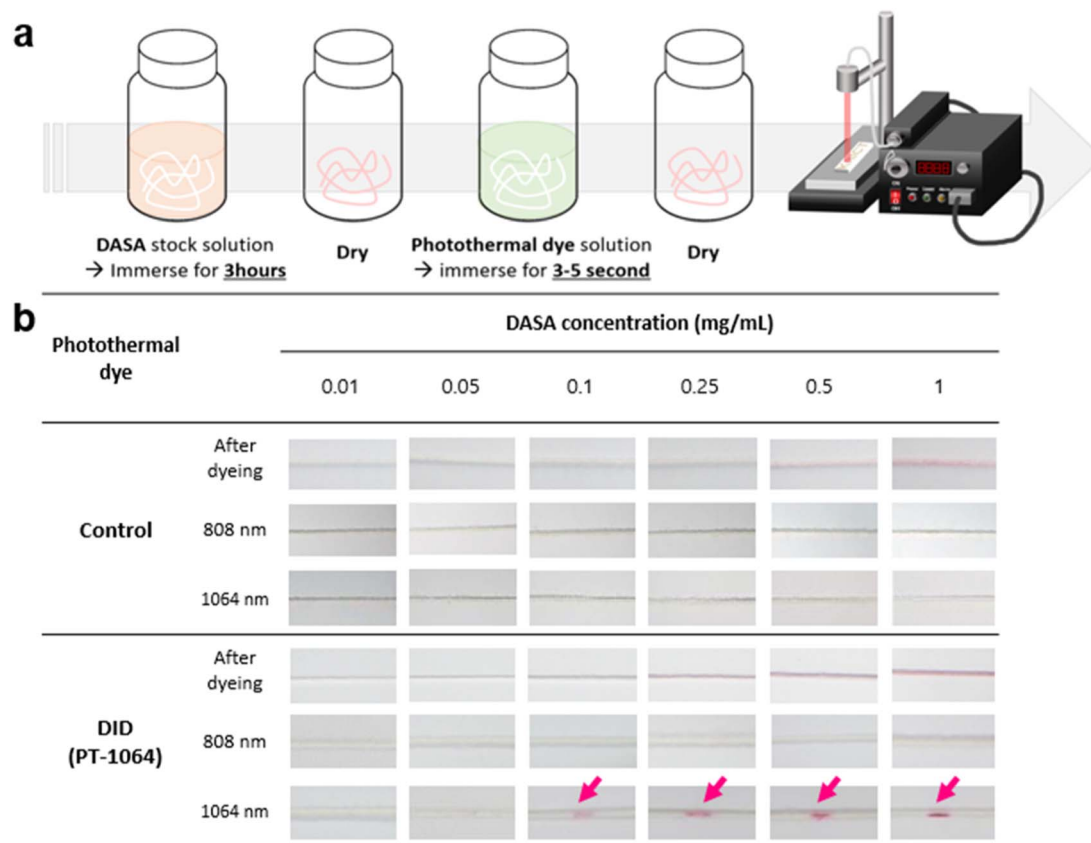
Fig. 4 (a) Overall dyeing process. (b) Responsiveness test results for selective wavelengths of security fibers fabricated through this study. (control: state in which photothermal dyes are not dyed, only thermochromic dyes are dyed, DID (PT-1064): after dyeing with thermochromic dyes, and then photothermal dyes are dipped).

after dyeing. To prepare the film, a mixed solution was prepared by adjusting the mass ratio of PMMA (M_w = 120 000): dye : toluene from 10 : 1 : 89 to 10 : 0.1 : 89.9. The prepared mixed solution was spin-coated at 3000 rpm for 30 s on a 2.5 × 2.5 slide glass washed using the following (in the same order): water, acetone, and chloroform. The samples were then oven-dried for 1 h. The NIR laser irradiated 15 cm away from the coated glass slide. The light irradiation intensity was fixed at 1 W and the laser diameter was fixed at 1.5 mm.

3. Results and discussion

3.1. Characterization of photothermal and thermochromic dyes

The absorption spectrum and photothermal effect of DID were measured as summarized in Fig. 2. Due to DID in a solid state after being introduced into the fiber, the photothermal performance of DID dispersed in the PMMA films was investigated. As shown in Fig. 2(a), DID exhibited a maximum absorption wavelength of over 1000 nm and almost no absorption in the vis region from 400–800 nm. The DID-coated film containing 0.1 wt% DID was highly transparent with transmittance values of 98.9% (Fig. S3†). The specific absorption of DID in the NIR region did not overlap with the absorption characteristics of commercial colorants, and DID is not expected to infringe on

the textile color after being introduced into the fiber. Upon irradiation of a 1064 nm laser (0.98 W), which is similar to the maximum absorption wavelength of DID, the surface temperature of the DID-coated film was increased to ~65 °C within 40 s (Fig. 2(b)). Moreover, when the film was irradiated with an 808 nm laser, which exhibited a weak absorption of DID, the surface temperature did not exceed 39 °C, thus indicating a high wavelength-selectivity of DID. Under 1064 nm laser irradiation, the DID film exhibited high stability during five repeated heating and cooling cycles with a similar temperature change (ΔT) of ~45 °C (Fig. 2(c)).

Donor–acceptor stannous ad is a thermochromic dye that exhibits the property of transitions from white (cyclic form) to red (linear form) upon exposure to heat, and subsequently regains its colorlessness when subjected to light, as shown in Fig. 3. As depicted in Fig. 3(a), a discernible shift in the maximum absorption wavelength of the DASA dye to 570 nm was observed with the application of heat, whereas the absorption wavelength shifted to 262 nm under light irradiation, excluding absorption in the vis range. To confirm the color change, even in the solid state, the reflectance when exposed to light or heat was measured using ellipsometry. The color of the DASA powder changed from white to red (14% reflectance at 520 nm) under heat exposure and from red to white (97% reflectance at 520 nm) when irradiated with white light (Fig. 3(b)). In
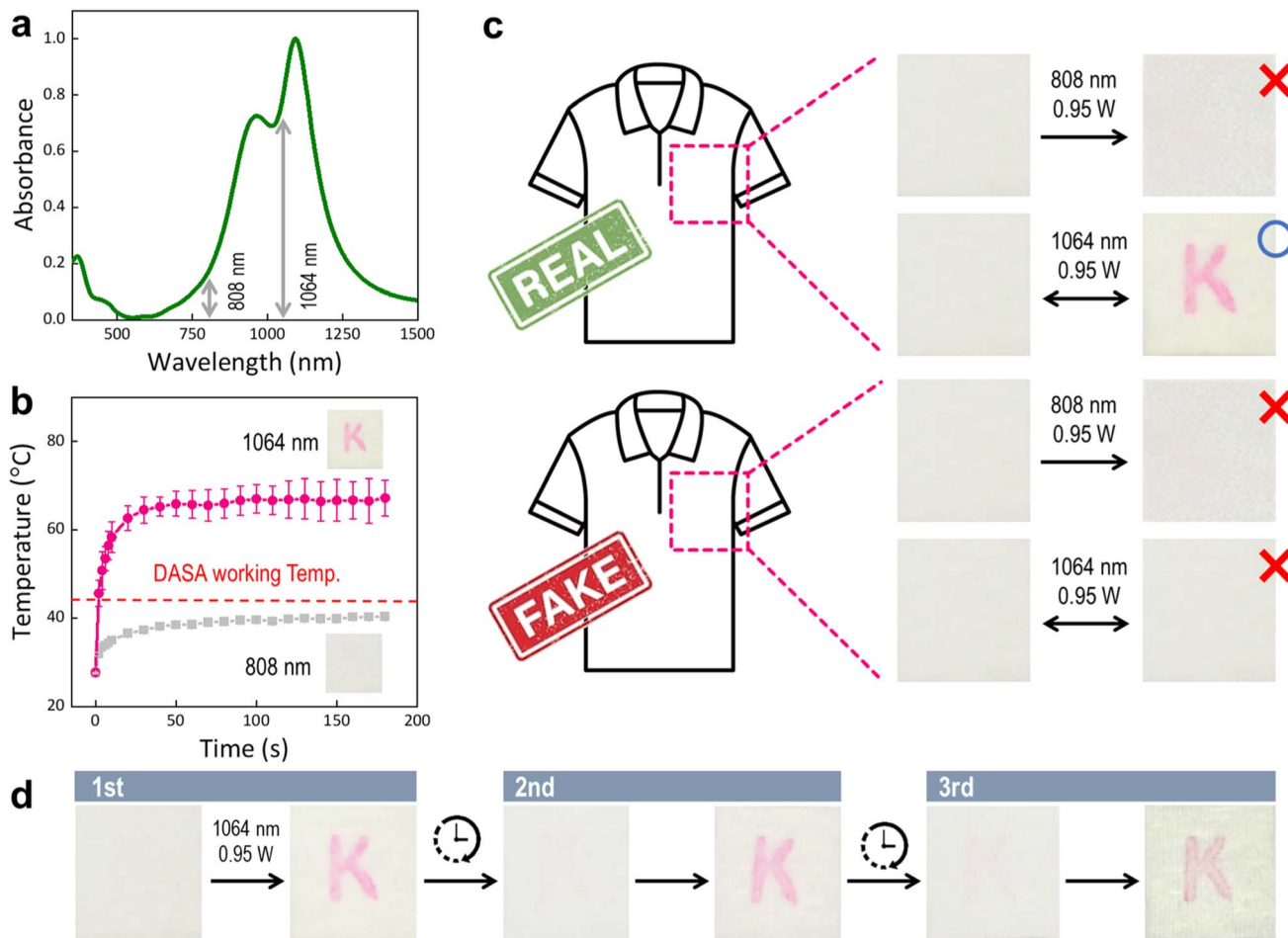
Fig. 5   (a) UV-vis absorption spectrum and (b) photo-thermal property of diimonium salt depend on NIR wavelength (808, 1064 nm) (c) simulated and physical images of the anti-counterfeit text label on clothes under 808, 1064 nm (d) repeatability anti-counterfeit text label under 1064 nm (color) and white light (colorless), respectively.

addition, the color change was repeated according to heat and white light, and was confirmed to be stable up to five times, as shown in Fig. 3(c). The inherent capacity of the DASA dyes to exhibit coloration under thermal stimulation can be achieved *via* photothermal conversion.

3.2.   Preparation of ACF fiber with response to NIR irradiation

The ACF system based on NIR region was first tested on cotton fibers, as shown in Fig. 4(a). First, cotton fibers of ~15 cm length were immersed in 0.01–1 mg L^{-1} DASA solution for 3 h each and dried. Then, DASA-stained fibers were dipped again in the DID dye solution and dried. The dipping time in the DID solution was within several seconds to prevent dissolution of DASA from the stained fibers. A series of DASA-stained fibers with and without photothermal dyes were irradiated with two NIR wavelengths: 808 nm and 1064 nm. As shown in Fig. 4(b), the fiber without the photothermal dye did not change color at either 808 nm or 1064 nm NIR wavelengths. However, in the presence of DID, DASA-stained fibers appeared red under 1064 nm irradiation, whereas they did not change color when irradiated with light at

808 nm due to the wavelength-specific absorption of DID. As a result, the concentration of the DASA solution for ACF fiber was optimized to 0.25 mg mL^{-1} to exhibit a clear color change. Despite the strong red color, fibers immersed in a DASA solution with >0.5 mg mL^{-1} started to appear reddish even when dried at room temperature without external stimulation, thus hindering the application of ACF fibers.

3.3.   Demonstration of ACF textile labels for brand protection

Finally, we implemented anti-counterfeit clothes with an alphabet K label that could distinguish between genuine from counterfeit products under irradiation at a specific NIR wavelength (Fig. 5). As shown in Fig. 5(a and b), the absorption intensity at 808 nm was greater than that at 1064 nm by a factor greater than 4.8 according to the NIR absorption wavelength of the photothermal dye, and the temperature change *via* photothermal effect was 39 °C and 65 °C at 808 nm and 1064 nm, respectively. Considering that DASA changed from colored to colorless by heat at 45 °C, this indicates that the color change of DASA can be controlled by selective NIR wavelength.

As shown in Fig. 5(c), it was confirmed that the anti-counterfeited fibers, including DASA and DID, did not change color at 808 nm; however, the letter K only appeared red at 1064 nm, thus indicating the implementation of a system that can discriminate genuine products at a specific NIR wavelength. However, in the case of a counterfeit product, there was no change at the 808 nm or 1064 nm NIR wavelengths because it contained only DASA and no photothermal dye. Due to this difference in absorption intensity and the photothermal effect, it is possible to check whether the DASA changes color according to the selection of the NIR wavelength. To assess whether ACF with wavelength selectivity can be repeatedly confirmed, as shown in Fig. 5(d), when repeated three times at 1064 nm, the letter K turned from colorless to red, and authenticity was confirmed. It was possible to return the colored label to colorless by simply storing the clothing without applying external stimulation. Therefore, a system capable of distinguishing between genuine and counterfeit products was successfully implemented in this study using the photothermal effect according to the wavelength of the NIR and discoloration dyes.

4. Conclusion

We designed a high-level ACF technology with NIR wavelength selectivity that can be visually confirmed with the naked eye using a thermochromic dye, i.e., a donor–acceptor Stenhouse adduct (DASA), and an NIR absorption dye (DID dye). Although NIR dyes exhibit clear absorption capacities in the NIR region, there is no absorption in the vis region; therefore, they exhibited transparent NIR absorption capacities. This advantage makes them suitable for application to fibers of various colors due to the non-overlap with the absorption characteristics of fibers of various colors. In particular, the temperature increase of the photothermal dye showed to 65 °C at 1064 nm and 39 °C at 808 nm within 40 s, respectively. Considering the temperature of DASA, the dye color changed from colorless to red at 45 °C. Moreover, it should be noted that the color change of DASA can be controlled by selective NIR wavelength. When applied to the brand identification system for textiles base on these results, we successfully implemented a system that can visually distinguish between genuine and counterfeit products at a specific wavelength of 1064 nm in NIR. It was confirmed that this ACF system functioned adequately even when repeated three times. The findings of this study therefore serve as a promising technology for the prevention of counterfeiting when verifying the authenticity of branded clothes.

Conflicts of interest

There are no conflicts to declare.

Acknowledgements

References

1 J. Andres, R. D. Hersch, J.-E. Moser and A.-S. Chauvin, *Adv. Funct. Mater.*, 2014, **24**, 5029.

2 N. Vahedigharehchopogh, O. Kıbrıslı, E. Erol, M. Ç. Ersundu and A. E. Ersundu, *J. Mater. Chem. C*, 2021, **9**, 2037.

3 J. Hu, S. Yang, Z. Chen, Y. Chen and J. Wei, *ACS Appl. Polym. Mater.*, 2023, **5**, 1002.

4 Y. Liu, F. Han, F. Li, Y. Zhao, M. Chen, Z. Xu, X. Zheng, H.-L. Hu, J. Yao, T. Guo, W. Lin, Y. Zheng, B. You, P. Liu, Y. Li and L. Qian, *Nat. Commun.*, 2019, 2409.

5 G. Vidotto, P. Anselmi, L. Filipponi, M. Tommasi and A. Saggino, *Front. Psychol.*, 2018, **9**, 1100.

6 A. A. Ansari, K. M. Aldajani, A. N. AlHazaa and H. A. Albrithen, *Coord. Chem. Rev.*, 2022, **462**, 214523.

7 Q. An, F. Zhang, Q. Sun, J. Wang, L. Li, J. Zhang, W. Tang and Z. Deng, *J. Mater. Chem. A*, 2015, **3**, 16653.

8 M. Tu, H. Reinsch, S. Rodrinuea-Hermida, R. Veerbeke, T. Stassin, W. Egger, M. Dickmann, B. Dieu, J. Hofkens, I. F. J. Vankelecom, N. Stock and R. Ameloot, *Angew. Chem., Int. Ed.*, 2019, **58**, 2423.

9 M. Wang, F. Li, Y. Lei, F. Xiao, M. Liu, S. Liu, X.-b. Huang, H. Wu and Q. Zhao, *Chem. Eng. J.*, 2022, **429**, 132288.

10 M. Han, B. Kim, H. Lim, H. Jang and E. Kim, *Adv. Mater.*, 2019, 1905096.

11 N. Ma, Y.-W. Jiang, X. Zhang, H. Wu, J. N. Myers, P. Liu, H. Jin, N. Gu, N. He, F.-G. Wu and Z. Chen, *ACS Appl. Mater. Interfaces*, 2016, **8**, 28480.

12 H. Xu, H. Deng, X. Ma, Y. Feng, R. Jia, Y. Wang, Y. Liu, W. Li, S. Meng and H. Chen, *J. Nanobiotechnol.*, 2023, **21**, 132.

13 B.-D. Zheng, Q.-X. He, X. Li, J. Yoon and J.-D. Huang, *Coord. Chem. Rev.*, 2021, **426**, 213548.

14 Y. Wang, G. Xia, M. Tan, M. Wang, Y. Li and H. Wang, *Adv. Funct. Mater.*, 2022, **32**, 2113098.

15 Y.-Y. Li, T. Wei, C. Liu, Z. Zhang, L.-F. Wu, M. Ding, S. Yuan, J. Zhu and J.-L. Zuo, *Eur. J. Chem.*, 2023, **29**, 34.

16 H. Liu, J. Yin, E. Xing, Y. Du, Y. Su, Y. Feng and S. Meng, *Dyes Pigm.*, 2021, **190**, 109327.

17 L. Kortekaas and W. R. Browne, *Chem. Soc. Rev.*, 2019, **48**, 3406.

18 B. Potaniec, M. Zdończyk and J. Cybińska, *Molecules*, 2022, **27**(10), 3092.

19 S. Helmy, F. A. Leibfarth, S. Oh, J. E. Poelma, C. J. Hawker and J. Fead de Alaniz, *J. Am. Chem. Soc.*, 2014, **136**, 8169.

20 M. M. Lerch, W. Szymanski and B. L. Feringe, *Chem. Soc. Rev.*, 2018, **47**, 1910.

21 B. F. Lui, N. T. Tierce, F. Tong, M. M. Sroda, H. Lu, J. Read de Alani and C. J. Bardeen, *Photochem. Photobiol. Sci.*, 2019, **18**, 1587.

© 2024 The Author(s). Published by the Royal Society of Chemistry